ARTICLES

Anomalous Dual Fluorescence of Benzanilide†

Frederick D. Lewis* and Timothy M. Long

Department of Chemistry, Northwestern University, Evanston, Illinois 60208-3113

Received: July 11, 1997; In Final Form: November 3, 1997

The absorption and fluorescence spectra of benzanilide and *N*-methylbenzanilide have been investigated in solution and low-temperature glasses and assigned with the aid of ZINDO calculations. The anomalous dual fluorescence observed by previous workers has been assigned to the two lowest singlet states of benzanilide. The lower energy n,π^* state is populated by excitation in the long-wavelength tail of the absorption band. Its fluorescence is readily detected in low-temperature glasses and at room temperature in aromatic solvents. Large NMR solvent-induced shifts provide evidence for ground-state complex formation of benzanilide with aromatic solvents. The higher energy π,π^* state is populated by excitation of an allowed transition. It undergoes twisting about the amide C−N bond to form a fluorescent twisted intramolecular charge-transfer state with a maximum of 520 nm in benzene solution. In rigid glasses twisting to form the twisted charge-transfer state cannot occur, and the π,π^* state undergoes internal conversion to the lower energy n,π^* state.

Assignment of the weak room-temperature luminescence of benzanilide (BA) has proven to be a formidable challenge. O'Connell et al.[1] initially reported that BA displays strongly overlapping fluorescence and phosphorescence in an EPA glass at 77 K but is nonfluorescent in ethanol solution. Kasha and co-workers[2] subsequently reported that BA displays dual fluorescence at room temperature in methylcyclohexane (MC) solution. The weaker fluorescence (F_1) has an approximate mirror-image relationship to the absorption spectrum and was attributed to a state of mixed n,π^* and π,π^* character.[2b] The stronger fluorescence (F_2) has a large Stokes shift and initially was assigned to the imidol tautomer, supposedly formed in a double proton transfer from a hydrogen-bonded dimer.[2a] Subsequent observation of similar Stokes-shifted emission for *N*-methylbenzanilide (MBA), which cannot undergo tautomerization, led to the suggestion that the F_2 fluorescence of MBA originated from a twisted intramolecular charge-transfer (TICT) state.[2b] The assignment of F_2 fluorescence of BA was then suggested to result from overlapping emission from a TICT state and the imidol tautomer. The TICT assignment for MBA and BA was supported by the observation of moderate solvent-induced shifts in alkane and ether solvents.[2b] The proposal of dual TICT and imidol F_2 fluorescence for BA was based on the bandwidth and the observation of dual-exponential F_2 fluorescence decay.[2c,d]

An investigation of the fluorescence of BA and MBA in MC solution by Azumaya et al.[3] led to the conclusion that the F_2 fluorescence of both molecules could be assigned to a single TICT state. Their study of various derivatives of BA and MBA with restricted geometries indicated that twisting about the amide C−N bond was a prerequisite for TICT formation. The requirement of geometric relaxation for TICT formation is consistent with the absence of Stokes-shifted fluorescence in a 77 K EPA glass.[1] Azumaya et al.[3] did not investigate the origin of the weak F_1 fluorescence of BA and MBA but noted that its intensity increased with time, possibly due to the formation of a fluorescent photoproduct.

Our interest in the structure and spectroscopy of aromatic carboxamides[4] prompted us to reinvestigate the nature of the singlet states of BA and MBA using a combination of spectroscopic and computational techniques. We find that both the F_1 and F_2 fluorescence of BA and MBA can be readily observed in aromatic solvents. The higher energy F_1 fluorescence is proposed to originate from the lowest energy singlet state, S_1, which is assigned to an amide-localized forbidden n $\rightarrow \pi^*$ transition. The lower energy F_2 fluorescence is assigned to a TICT state generated via twisting of a higher energy vertical excited state, S_2, which is populated via an allowed $\pi \rightarrow \pi^*$ transition. Internal conversion from S_2 to S_1 competes with twisting at low temperature but not at room temperature.

Experimental Section

Materials. BA (Aldrich) was recrystallized from ethanol prior to use. MBA was prepared by the reaction of benzoyl chloride with *N*-methylaniline in the presence of triethylamine. No impurities were detected by gas chromatography or ^{1}H NMR spectroscopy. Methylcyclohexane (Aldrich, anhydrous) and toluene (Fischer, ACS grade) were used as received. Benzene was distilled over sodium metal prior to use.

Methods. ^{1}H NMR spectra were measured using a Varian Gemini 300 spectrometer. UV−vis absorption spectra were obtained using a Hewlett-Packard 8542A diode array spectrophotometer using a 1 cm path quartz cell. Fluorescence spectra of degassed solutions (N_2) were recorded with a SPEX Fluoromax spectrometer. Low-temperature emission spectra were obtained using a liquid nitrogen cooled fluorescence Dewar with

† Dedicated to Nicholas J. Turro, postdoctoral mentor extraordinary, on the occasion of his 60th birthday.

S1089-5639(97)02259-7 CCC: $15.00
Published on Web 01/30/1998

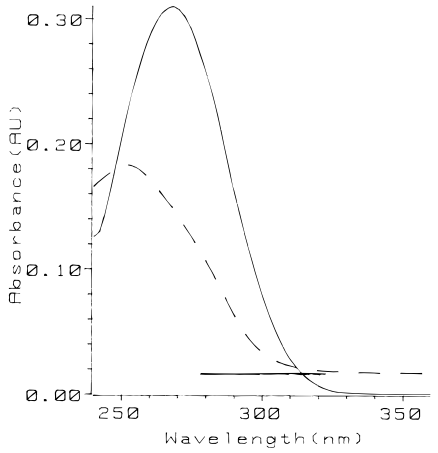

Figure 1. Absorption spectra of 2.0×10^{-5} M BA (—) and 2.6×10^{-5} M MBA (- - -) in methylcyclohexane solution. The baseline for MBA is displaced upward for clarity.

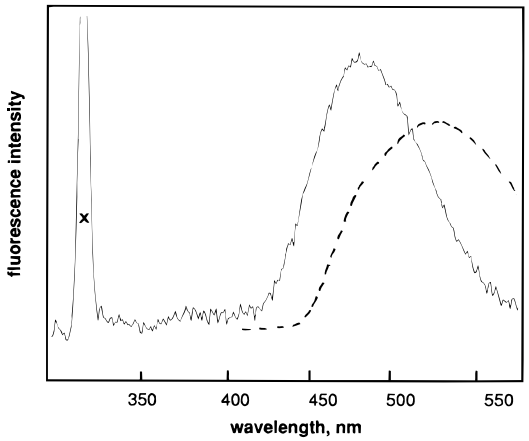

Figure 2. Fluorescence spectra of 2.0×10^{-5} M BA (—) and 2.6×10^{-5} M MBA (- - -) in methylcyclohexane solution at 293 K (λ_{ex} = 290 nm, X = scatter).

a hanging finger window or a Oxford Instruments variable temperature cryostat model DN1704 controlled with a model ITC4 temperature controller. Fluorescence quantum yields were determined using phenanthrene ($\Phi_f = 0.14$) as a reference standard.[5a] The integrated fluorescence intensity of the benzanilide and standard were compared for solutions with equal absorbance at the excitation wavelength. The estimated error in the measured quantum yields is ±20%. Fluorescence decays were measured on a Photon Technology International LS-1 single-photon-counting apparatus with a gated hydrogen arc lamp using a scatter solution to profile the lamp decay. Decays were analyzed using deconvolution and single-exponential or multiexponential least-squares fitting as described by James et al.[5b] Goodness of fit was judged by reduced χ^2 values (<1.2 in all cases), the randomness of residuals, and the autocorrelation function.

Minimum-energy conformations were calculated using a MM2 type force field as supplied in the Chem 3D software package (Chem 3D Plus, Cambridge Scientific Computing, Inc., Version 3.2) for a Power Macintosh 7600/120 computer or in the CACHe program (Cache Scientific, version 3.6). The calculations of electronic structure and absorption spectra were performed using the semiempirical INDO/S-SCF-CI (ZINDO) algorithm developed by Zerner and co-workers.[6] The ZINDO calculations were performed using CACHe 3.6. The calculation was carried out in two steps. First, the ground state was calculated using MM2 minimized initial geometries to acquire molecular orbital coefficients and eigenvalues. This was followed by configuration interaction (CI) calculations, in which 9−12 filled and 9−12 unfilled orbitals were used. For the calculation of vertical transitions as a function of amide C−N dihedral angle, the ground-state structure was rotated about the appropriate bond and the CI calculation performed without reminimization of the complete structure.

Results

Electronic Spectra. The absorption spectra of BA and MBA in MC solution are shown in Figure 1. As previously reported by Kasha and co-workers,[2] both spectra consist of a single broad band with maxima at 268 and 252 nm for BA and MBA, respectively, and with tailing at long wavelengths. Only minor changes in the absorption maxima or extinction coefficients are observed in more polar solvents such as tetrahydrofuran or acetonitrile. Since the long-wavelength tail assumes importance in our fluorescence studies, extinction coefficients at 330 nm in MC solution were determined to be 80 and 20 M^{-1} cm^{-1} for BA and MBA, respectively. The appearance and intensity of the long wavelength tail are similar in more polar solvents and in the aromatic solvents benzene and toluene.

The fluorescence spectra of 2×10^{-5} M BA and MBA in MC solution are shown in Figure 2. The spectra display maxima at 475 and 515 nm, respectively, similar to those assigned to the F_2 band by Kasha and co-workers.[2] The position of this broad fluorescence band is independent of excitation wavelength (280−330 nm), and the fluorescence excitation spectrum is similar to the absorption spectrum ($\lambda_{max} \sim 270$ nm for BA), as observed by Azumaya et al.[3] The fluorescence at ca. 330 nm assigned to the F_1 band by Kasha and co-workers[2] is absent in freshly prepared solutions but increases in intensity upon exposure to light, as observed by Azumaya et al.[3] The 330 nm band most likely is due to a photoproduct (see Discussion section).

The F_2 fluorescence maxima of BA and MBA are red-shifted in benzene solution to 510 and 540 nm, respectively. The excitation maximum for F_2 fluorescence is ∼310 nm due to competitive absorption by solvent at shorter wavelengths. Excitation of a 3×10^{-3} M solution of BA in the long-wavelength tail of its absorption spectrum results in fluorescence emission with a maximum at 433 nm which we assign as F_1 fluorescence (Figure 3). The excitation maximum for F_1 fluorescence is 340 nm. Excitation at progressively shorter wavelengths results in a decrease in the F_1 fluorescence and an increase in the F_2 fluorescence intensity. Similar excitation-wavelength-dependent dual fluorescence was observed for MBA in benzene solution and for both BA and MBA in toluene solution. Exposure to light results in an increase in 330 nm fluorescence but not the 433 nm fluorescence. Attempts to observe F_1 fluorescence in several other solvents, including MC, dibutyl ether, dioxane, tetrahydrofuran, and acetonitrile, were unsuccessful even when high concentrations of BA ($>10^{-3}$ M) were used. Competitive absorption between 300 and 340 nm precludes the use of more polar aromatic solvents such as chlorobenzene and benzonitrile.

The emission spectra of BA at several temperatures in 1:1 MC−toluene are shown in Figure 4. Only long wavelength 505 nm emission is observed at room temperature in MC−toluene solution (Figure 4). At 193 K, which is above the glass transition temperature (T_g), only shorter wavelength 434 nm emission is observed. At 77 K (below T_g) the spectrum is slightly broader and more intense than at 193 K. As previously reported by O'Connell et al.,[1] no emission is observed at room

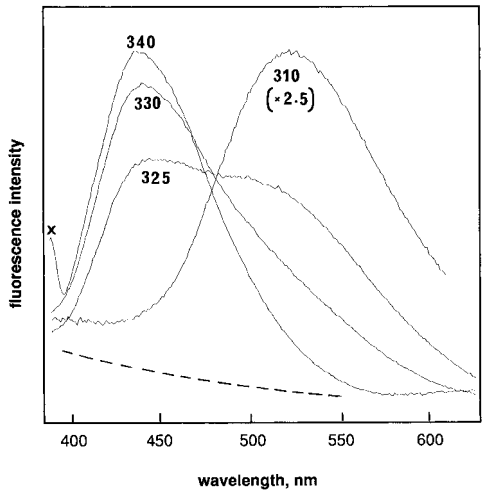

Figure 3. Fluorescence spectra of 3×10^{-3} M BA in benzene solution with $\lambda_{ex} = 310$ (×2.5), 325, 330, and 340 nm (X = scatter). Baseline indicated by a dashed line.

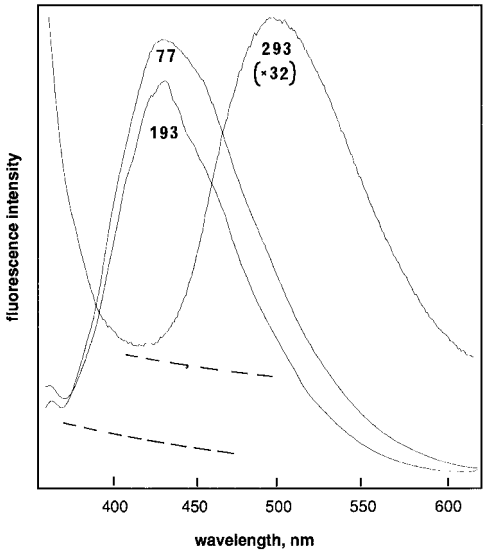

Figure 4. (a) Fluorescence spectra of BA in MC−toluene solution at 293 (×32), 193, and 77 K ($\lambda_{ex} = 320$ nm). Baselines indicated by dashed lines.

temperature in EPA solution. Long-wavelength 501 nm emission is observed at 110 K (above T_g) and short-wavelength 429 nm emission at 77K (below T_g) in EPA.

Fluorescence quantum yields (Φ_f) and decay times (τ) were measured for BA and MBA in MC and benzene solution (Table 1). Values of Φ_f for F_2 fluorescence are in the range $(3-6) \times 10^{-4}$ M in both solvents. A larger value is obtained for the F_1 fluorescence in 3×10^{-3} M benzene solution. Fluorescence decays for BA and MBA were determined in benzene solution using a single-photon-counting apparatus with a time resolution of approximately 0.2 ns. The decays were deconvoluted using a single or multiple least-squares analysis, as described by James et al.[5b] Decays were best fit by a biexponential function with short- and long-lived decay components. No rising components were detected for either F_1 or F_2 fluorescence. The F_2 fluorescence of both BA and MBA was dominated by the short-lived components reported in Table 1, along with the values reported by Azumaya et al.[5] for MC solution. The F_1 fluorescence of MBA was also dominated by the short-lived component; however, the long-lived component has a significant preexponential in the case of BA. Attempts to determine decay times in low-temperature glasses were unsuccessful due to a combination low fluorescence intensity and low efficiency of the optical Dewar when used with the single-photon-counting apparatus.

TABLE 1: Fluorescence Emission Maxima, Quantum Yields, and Lifetimes

amide, emission	solvent	λ_{ex}, nm[a]	λ_{max}, nm[b]	$10^3\Phi_f$[c]	τ, ns (A)[d]
BA, F_2	MC	290	475	0.6	0.86[e]
BA, F_2	benzene	310	510	0.4	1.0 (0.99)
BA, F_1	benzene	340	433	7.0	2.1 (0.83)[f]
MBA, F_2	MC	290	515	0.4	1.7 (0.96)[e]
MBA, F_2	benzene	310	540	0.3	2.1 (0.98)
MBA, F_1	benzene	340	435	1.0	1.0 (0.98)

[a] Excitation wavelength used for fluorescence quatum yield and lifetime measurements. [b] Maximum intensity of fluorescence band. [c] Fluorescence quantum yield. Estimated error ±20%. [d] Preexponential for major decay component. [e] Data from ref 3. [f] Second component has a lifetime of 9.5 ns and a preexponential of 0.17.

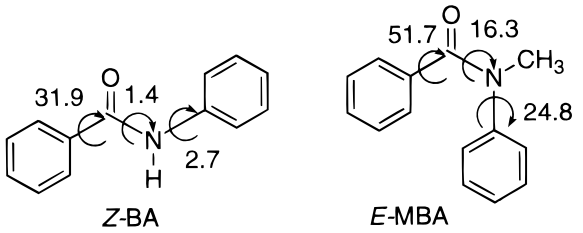

Figure 5. Calculated dihedral angles for *Z*-BA and *E*-MBA.

TABLE 2: ^{1}H NMR Aromatic Solvent-Induced Shifts for BA

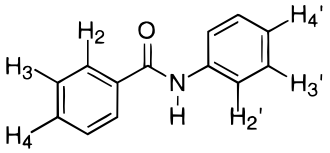

^{1}H	δ_{CDCl_3} (ppm)[a]	$\delta_{C_6D_6}$ (ppm)	$\Delta\delta$ ($\delta_{C_6D_6} - \delta_{CDCl_3}$)
2	7.88	7.61	−0.27
3	7.49	7.08	−0.41
4	7.56	7.11	−0.45
2′	7.64	7.58	−0.06
3′	7.38	6.97	−0.41
4′	7.16	6.92	−0.24

[a] Data from ref 7a.

Ground-State Structure. The ground-state structures of BA and MBA in solution and in the solid state have been investigated by Shudo and co-workers.[7] According to their ^{1}H NMR assignments, BA exists predominantly as the *Z* conformer and MBA as the *E* conformer in $CDCl_3$ solution (Figure 5). We have assigned the NMR spectra of BA and MBA in C_6D_6 solution by analogy to the assignments of Itai et al.[7a] Chemical shift values for BA in $CDCl_3$ and C_6D_6 solution are summarized in Table 2, along with the aromatic solvent-induced shift (ASIS)[8] for each aromatic proton. Similar negative (upfield) shifts are seen for the aromatic protons of MBA.

Dihedral angles obtained from MM2 calculations for *Z*-BA and *E*-MBA (unsolvated molecules) are summarized in Figure 5. The calculated ground-state amide dihedral angles for *Z*-BA and *E*-MBA are similar to those reported for their crystal structures.[7] The calculated energy of *E*-BA is ∼5 kcal/mol higher than that of *Z*-BA, and the calculated barrier to rotation is 18 kcal/mol. This barrier is similar to that determined from temperature-dependent NMR data for *N*,*N*-dimethylbenzamide.[9] The calculated energy of *Z*-MBA is ∼1 kcal/mol lower than that of *E*-MBA, and the calculated barrier to rotation is 9 kcal/

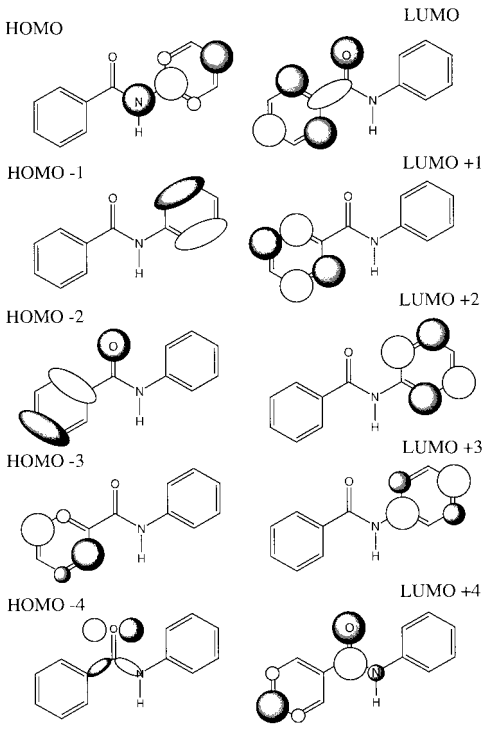

Figure 6. Frontier molecular orbitals for BA (HOMO−4 is lowest in energy and LUMO+4 highest in energy).

TABLE 3: Calculated Dipole Moments, Absorption Maxima, Oscillator Strengths, and Character of the Singlet States of Benzanilide

singlet	μ, D	λ_{max}, nm	f	CI (%) and character[a]
S_0	5.3			
S_1	5.5	375.1	0.0005	73.7 HOMO−4 → LUMO
				21.2 HOMO−4 → LUMO+4
S_2	17.0	289.7	0.43	84.9 HOMO → LUMO
				3.5 HOMO → LUMO+2
				2.9 HOMO → LUMO+3
				2.6 HOMO → LUMO+4

[a] Benzanilide frontier orbitals shown in Figure 6.

mol. Preferential solvation of the *E* conformer could reverse the relative energies in solution. The lower barrier for MBA vs BA may result from ground-state repulsion between the two benzene rings in both the *E* and *Z* conformers (Figure 5).

ZINDO Calculations. The electronic structure and spectra of BA and MBA were investigated by semiempirical INDO/S-SCF-CI (ZINDO) calculations using the algorithm developed by Zerner and co-workers.[6] The molecular structures were those obtained from MM2 calculations. The nodal patterns for the five highest occupied and lowest unoccupied molecular orbitals of BA are shown in Figure 6. The HOMO-4 and LUMO+4 orbitals are amide-localized, whereas the other frontier orbitals are largely localized on either the benzoyl or aniline portions of the molecule. The calculated absorption maxima, oscillator strengths, dipole moments, and character of the three lowest energy singlet states of BA are summarized in Table 3. The lowest energy singlet state is largely n,π* (amide → benzoyl) in character and possesses a very low oscillator strength. The second singlet state is largely π,π* (aniline → benzoyl) in character and possesses a large oscillator strength. The calculated dipole moment of S_2 is significantly larger than that of S_0 or S_1. The next three lowest energy singlet states are also π,π* in character (S_3 is largely aniline → aniline and S_4 and S_5 are largely benzoyl → benzoyl).

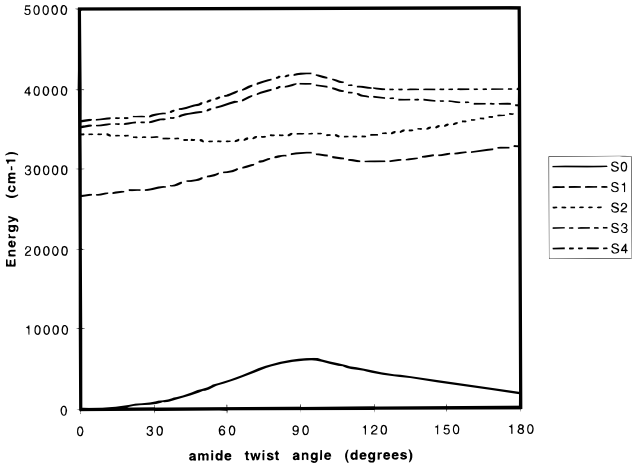

Figure 7. Calculated potential energy surfaces for amide C−N rotation in BA (0° is *Z* isomer and 180° is *E* isomer).

ZINDO calculations have also been performed for MBA. The frontier π orbitals of MBA are delocalized over both the benzoyl and aniline groups, and the singlet states display more extensive configuration interaction than is the case for BA. The first singlet of MBA is largely n,π* in character. The lowest energy state of MBA with largely π,π* character is S_4. It is calculated to lie at higher energy (279 nm) and have a lower oscillator strength (0.17) than S_2 for BA (Table 3).

Since rotation about the amide C−N bond has been implicated in the formation of the singlet state responsible for F_2 fluorescence, we have investigated the effect of this bond rotation on the energies of the lowest singlet states of BA. Vertical transitions were calculated at 15° increments of rotation about this bond, using the MM2 minimized geometries. The calculated ground-state energies were added to the vertical transitions, and potential energy surfaces were generated using Microsoft Excel 5.0 to interpolate and produce smooth fits to the data. As shown in Figure 7, the calculated barrier for rotation of S_1 (16 kcal/mol) is similar to that calculated by MM2 for ground-state rotation. In contrast, there is no barrier for rotation of S_2. Analogous calculations for MBA produced similar potential energy surfaces with a barrier of 14.7 kcal/mol for rotation of S_1 and no barrier for rotation of S_4.

Discussion

Previous investigations of the photophysics of BA and MBA have left unresolved questions concerning the identity of the excited states responsible for both the Stokes-shifted fluorescence and the shorter wavelength fluorescence, labeled F_2 and F_1, respectively, by Kasha and co-workers.[2] F_2 fluorescence was originally attributed to adiabatic formation of the tautomeric imidol[2a] but later reattributed to a TICT state.[2b,3] F_1 fluorescence was attributed by Kasha to a Franck−Condon (FC) singet state that rapidly relaxes to the TICT state.[2d] Azumaya et al.[3] noted that the intensity of the very weak F_1 emission increased upon exposure to light and might arise from a photoproduct. Aniline, which is formed with a quantum yield of 1×10^{-3} upon irradiation of BA in ethanol solution,[10a] appears to be a likely candidate for the F_1 fluorescence previously observed in MC solution. BA also undergoes photo-Fries rearrangement[10a] and photocyclization to phenanthridones; however, these products do not fluoresce in the region of F_1 fluorescence.[10b]

An impediment to the investigation of the excited states of BA and MBA is their very weak fluorescence. We find that the F_2 fluorescence quantum yields are $\sim 5 \times 10^{-4}$ in the

nonpolar solvents MC and benzene (Table 1). Increasing solvent polarity results in a decrease in fluorescence intensity, and fluorescence has not been detected in solvents more polar than tetrahydrofuran. We are unable to detect F_1 fluorescence from freshly prepared solutions of recrystallized BA in MC (Figure 2) and other nonaromatic solvents. However, dual fluorescence can readily be observed in aromatic solvents (Figure 3). In benzene solution the F_2 fluorescence has an emission maximum similar to that reported by Heldt et al.[2b] for ether solvents. Benzene and diethyl ether have very similar values of $E_T(30)$, the Dimroth−Reichardt solvent polarity parameter.[11]

The most striking result of the present investigation is the observation of significantly enhanced F_1 fluorescence upon excitation of BA and MBA at long wavelengths (>310 nm) in aromatic solvents (Figure 3). Because of the low intensity of the long-wavelength absorption (Figure 1), the use of higher concentrations facilitates the observation of F_1 fluorescence in aromatic solvents, but not in nonaromatic solvents such as MC. The quantum yield and lifetime for F_1 fluorescence in benzene solution are larger than those for F_2 fluorescence (Table 1). Heldt et al.[2d] reported a lifetime of 12 ps for the Franck−Condon singlet state of BA in MC solution, as determined by transient absorption spectroscopy. Assuming that the same state is responsible for F_1 fluorescence, the longer lifetime in benzene vs MC solution could account for its much stronger fluorescence in benzene.

The enhanced intensity of F_1 fluorescence in aromatic solvents presumably results from solvent perturbation of the radiative or nonradiative decay rates. Solvent perturbation of radiative decay is noticeable only when the transition moment of the unsolvated molecule is very small,[12] as is the case for the n,π^* state of BA in nonaromatic solvents. Evidence for ground-state interaction of BA with aromatic solvents is provided the large differences in ^{1}H NMR chemical shifts in aromatic vs nonaromatic solvents (Table 2). Aromatic solvent-induced shifts (ASIS) for amides were first reported by Hatton and Richards,[13] who attributed them to formation of a π complex in which protons near the amide functional group lie in the shielding region of the aromatic solvent. Amide ASIS data have been used to assign the conformation of tertiary amides.[9,14] Ground-state interaction between aromatic solvents and porphyrins results in selective enhancement of solvent Raman bands via resonance vibrational coupling.[15] We suspect that similar coupling is responsible for the enhanced radiative decay of the n,π^* state of BA in aromatic solvents which results in the observation of F_1 fluorescence.

The observation of F_1 fluorescence upon long-wavelength excitation and F_2 fluorescence upon short-wavelength excitation of BA (Figure 3) requires that emission occurs from two different singlet states that do not interconvert. Heldt et al.[2b] proposed that a forbidden transition of mixed n → π^* and π → π^* character is buried under the allowed π → π^* transition, which dominates the absorption spectra of BA and MBA (Figure 1). In acetanilide the n → π^* transition is resolved from the higher energy π → π^* transition.[16] The results of our ZINDO calculations (Table 3) are consistent with the presence of an amide-localized forbidden n → π^* transition at lower energy than the first allowed π → π^* transition for both BA and MBA. In the case of BA the allowed π → π^* transition is predominantly aniline HOMO→benzoyl LUMO in character, whereas for MBA there is more extensive configuration interaction. The calculated oscillator strength for the π → π^* transition of BA is larger than that for MBA and the calculated energy of this transition is lower for BA, in accord with the appearance of their absorption spectra (Figure 1).

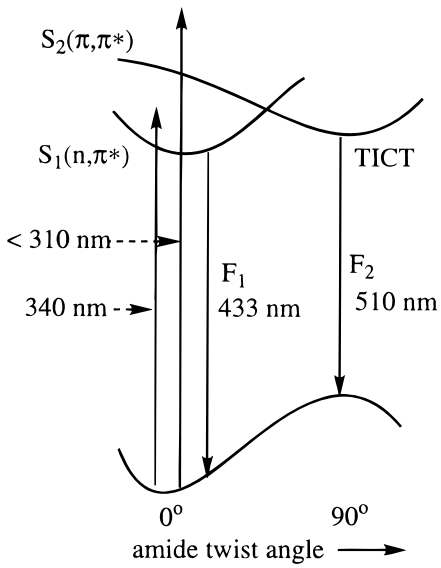

Figure 8. State diagram for BA.

A singlet-state diagram that can account for the anomalous fluorescence behavior of BA is shown in Figure 8. The F_1 fluorescence observed upon excitation in the long-wavelength tail of the absorption band in aromatic solvents (Figure 3) is attributed to an amide-localized lowest singlet (S_1) n,π^* state. The forbidden nature of this transition is consistent with its weak absorption and fluorescence. The absence of F_2 fluorescence upon long-wavelength excitation indicates that S_1 is not a precursor of F_2 fluorescence. Excitation of the allowed π → π^* transition results in the observation of F_2 fluorescence. However, several lines of evidence indicate that the FC S_2 state is not fluorescent. As noted Kasha and co-workers,[2] the large Stokes shift for F_2 fluorescence is indicative of a large change in geometry prior to fluorescence. In addition, the absence of F_2 fluorescence both in rigid glasses and for geometrically constrained analogues of BA[3] indicates that a substantial geometric change is necessary for the observation of F_2 fluorescence. The solvent-induced shift in the fluorescence maxima[2b] supports the assignment of F_2 to a TICT state.

Azumaya et al.[3] have proposed that twisting about the amide C−N bond in BA and MBA is required for the formation of the TICT state responsible for F_2 fluorescence. Rigid analogues of BA in which this torsion is inhibited are either nonfluorescent or very weakly fluorescent. Twisting about the amide C−N bond is also responsible for the *E*,*Z* photoisomerization of simple aliphatic amides.[17] Our investigation of the potential energy surface for amide C−N twisting in BA and MBA indicates that barriers exist in the ground state and S_1, but not for S_2 (Figure 7). A low barrier for amide rotation of the S_2 FC singlet state to form the TICT state could explain the absence of internal conversion of S_2 to S_1 in solution at room temperature. Lowering the temperature of a MC−toluene solution of BA from 273 to 193 K results in a change from F_2 to F_1 fluorescence (Figure 4). Further cooling to 77 K results in only modest changes in emission intensity and band shape, which is similar to that for F_1 fluorescence in benzene solution.

Observations of dual fluorescence have frequently been attributed to emission from two excited states: short-wavelength fluorescence originating from a state of geometry similar to that of the FC excited state and long-wavelength emission to a TICT state with relaxed geometry.[18−20] In the case of 4-(dimeth-

ylamino)benzonitrile formation of the TICT state is proposed to occur via the relaxed FC state.[18] Wintgens et al.[20] have recently suggested that the dual fluorescence of *N*-phenyl-2,3-naphthalimides results from the formation of two singlet states that are not kinetically connected from a single FC excited state. The dual fluorescence of BA is unique in that the lowest singlet S_1 yields only the higher energy F_1 fluorescence, whereas the higher energy FC S_2 state is the precursor of the lower energy F_2 TICT fluorescence (Figure 8). This seeming anomaly is attributed to a decrease in the S_2 energy and increase in S_0 energy upon twisting of the amide C−N bond, resulting in a lower energy for the TICT state than for the planar S_1. $S_2 \rightarrow S_1$ internal conversion does not occur in fluid solution at room temperature but does occur at low temperature in MC/toluene solution and in several rigid glasses. Formation of the TICT state from S_1 is not observed under any conditions, and the observation of S_1 fluorescence requires the use of either aromatic solvents or low temperatures.

Acknowledgment. Financial support for this research has been provided by the National Science Foundation. T.M.L. thanks Northwestern University for an undergraduate scholarship and the Marple-Schwitzer Award. We thank Jye-Shane Yang for helpful advice.

References and Notes

(1) O'Connell, E. J.; Delmauro, M.; Irwin, J. *J. Photochem. Photobiol.* **1971**, *14*, 189.

(2) (a) Tang, G.-Q.; MacInnis, J.; Kasha, M. *J. Am. Chem. Soc.* **1987**, *109*, 2531. (b) Heldt, J.; Gormin, D.; Kasha, M. *Chem. Phys. Lett.* **1988**, *150*, 433. (c) Heldt, J.; Gormin, D.; Kasha, M. *J. Am. Chem. Soc.* **1988**, *110*, 8255. (d) Heldt, J.; Gormin, D.; Kasha, M. *Chem. Phys.* **1989**, *136*, 321.

(3) Azumaya, I.; Kagechika, H.; Fujiwara, Y.; Itoh, M.; Yamaguchi, K.; Shudo, K. *J. Am. Chem. Soc.* **1991**, *113*, 2833.

(4) (a) Lewis, F. D.; Burch, E. L. *J. Phys. Chem.* **1996**, *100*, 4055. (b) Lewis, F. D.; Yang, J.-S. *J. Phys. Chem. B* **1997**, *101*, 1775.

(5) (a) Birks, J. B. *Photophysics of Aromatic Molecules*; Wiley-Interscience: London, 1970; p 128. (b) James, D. R.; Siemiarczuk, A.; Ware, W. R. *Rev. Sci. Instrum.* **1992**, *63*, 1710.

(6) (a) Bacon, A. D.; Zerner, M. C. *Theor. Chim. Acta* **1970**, *53*, 21. (b) Zerner, M. C.; Loew, G. H.; Kirchner, R. R., Mueller-Westerhoff, U. T. *J. Am. Chem. Soc.* **1980**, *102*, 589.

(7) (a) Itai, A.; Toriumi, Y.; Tomioka, N.; Kagechika, H.; Azumaya, I.; Shudo, K. *Tetrahedron Lett.* **1989**, *30*, 6177. (b) Itai, A.; Toriumi, Y.; Saito, S.; Kagechika, H.; Shudo, K. *J. Am. Chem. Soc.* **1992**, *114*, 10649. (c) Azumaya, I.; Kagechika, H.; Yamaguchi, K.; Shudo, K. *Tetrahedron* **1995**, *51*, 5277.

(8) (a) Jauquet, M.; Laszlo, P. In *Techniques of Chemistry*; Dack, M. R. J., Ed.; Wiley: New York, 1975; Vol. VIII, p 233. (b) Reichardt, C. *Solvents and Solvent Effects in Organic Chemistry*; VCH: Weinheim, Germany, 1990; p 311.

(9) Stewart, W. E.; Siddall, III, T. H. *Chem. Rev.* **1970**, *70*, 517.

(10) (a) Carlsson, D. J.; Gan, L. H.; Wiles, D. M. *Can. J. Chem.* **1975**, *53*, 2337. (b) Grimshaw, J.; de Silva, A. P. *J. Chem. Soc., Perkin Trans. 2* **1982**, 857.

(11) Reference 8b, p 363.

(12) (a) Durocher, G.; Sandorfy, C. *J. Mol. Spectrosc.* **1966**, *20*, 410. (b) Liptay, W. *Angew. Chem., Int. Ed. Engl.* **1969**, *8*, 177. (c) Michl, J.; Bonacic-Koutecky, *Electronic Aspects of Organic Photochemistry*, Wiley-Interscience: New York, 1990; p 75.

(13) (a) Hatton, J. V.; Richards, R. E. *Mol. Phys.* **1960**, *3*, 253. (b) Hatton, J. V.; Richards, R. E. *Mol. Phys.* **1962**, *5*, 139.

(14) Lewin, A. H.; Frucht, M. *Org. Magn. Reson.* **1975**, *7*, 206.

(15) Kincaid, J. R.; Proniewicz, L. M.; Bajor, K.; Bruha, A.; Nakamoto, K. *J. Am. Chem. Soc.* **1985**, *107*, 6774.

(16) (a) Baba, H.; Suzuki, S. *J. Chem. Phys.* **1960**, *32*, 1706. (b) Decoret, C.; Tinland, B. *Spectrosc. Lett.* **1971**, *4*, 263.

(17) Song, S.; Asher, S. A.; Krimm, S.; Shaw, K. D. *J. Am. Chem. Soc.* **1991**, *113*, 1155.

(18) Rettig, W. *Angew. Chem., Int. Ed. Engl.* **1986**, *25*, 971.

(19) For an alternative explanation see: Zachariasse, K. A.; Grobys, M.; Von Der Haar, Th.; Hebecker, A.; Il'ichev, Yu. V.; Kühnle, W.; Morawski, O. *J. Inf. Rec. Mater.* **1996**, *22*, 553.

(20) Wintgens, V.; Valat, P.; Kossanyi, J.; Demeter, A.; Biczók, L.; Bérces, T. *J. Photochem. Photobiol. A* **1996**, *93*, 109.